Sustainable Energy & Fuels

Aqueous Vanadium Complex for the Superior Electrolyte of a Thermo-Electrochemical Cell

Journal:	*Sustainable Energy & Fuels*
Manuscript ID	SE-COM-06-2023-000774.R2
Article Type:	Communication
Date Submitted by the Author:	04-Oct-2023
Complete List of Authors:	Yamada, Teppei; The University of Tokyo, Department of Chemistry, Faculty of Science Kobayashi, Takashi; Kyushu Daigaku Wakayama, Yusuke; The University of Tokyo, Department of Chemistry, Faculty of Science Matoba, Fumitoshi; The University of Tokyo, Department of Chemistry, Faculty of Science Yatsuzuka, Koichi; Kyushu Daigaku Kimizuka, Nobuo; Kyushu University - Ito Campus, Chemistry and Biochemistry Zhou, Hongyao; The University of Tokyo, Chemistry

COMMUNICATION

Aqueous Vanadium Complex for the Superior Electrolyte of a Thermo-Electrochemical Cell

Teppei Yamada*[a], Takashi Kobayashi[b], Yusuke Wakayama[a], Fumitoshi Matoba[a,b], Koichi Yatsuzuka[c], Nobuo Kimizuka[b], Hongyao Zhou[a]

Received 00th January 20xx,
Accepted 00th January 20xx

DOI: 10.1039/x0xx00000x

The Seebeck coefficient of a thermo-electrochemical cell consisting of vanadium complexes reaches −3.2 mV K^{-1} in water and −3.8 mV K^{-1} in a mixed solvent. The solvation entropy of the proton achieves the high S_e. The ZT and electrochemical cooling effect outperform that of the benchmark electrolyte, $[Fe(CN)_6]^{3-/4-}$.

Energy harvesting technology is one of the most significant issues for our sustainable future society because the effective use of primary energy can reduce CO_2 emissions. For waste-heat harvesting, thermo-electrochemical cells (TECs) are an alternative to semiconductor thermoelectrics.[1–3] TECs are liquid thermoelectric conversion devices. Thanks to recent developments in electrolytes[4], electrodes[5–7], redox species[4,8–17], redox systems[18,19], and thermoresponsive phenomena[20–24], a drastic improvement in the thermoelectric conversion efficiency has been made. In addition, the integration with the flow system[18,19] paves the way for their practical application. Hexacyanoferrate (II/III) ($[Fe(CN)_6]^{3-/4-}$) shares a dominant role as a redox couple used in TECs.[8,9,11] They have small ionic radii and high charge states, increasing the hydration entropies. The redox reaction of $[Fe(CN)_6]^{3-/4-}$ significantly changes the hydration entropy and results in the high Seebeck coefficient (S_e) of −1.4 mV K^{-1}. The high solubility of $[Fe(CN)_6]^{3-/4-}$ ions also leads to the high carrier concentration, ionic conductivity, and high figure-of-merit (*ZT*) of the TECs. Recently, the addition of chaotropic reagents was reported to induce a drastic increase in S_e.[7]

For the further development of TECs, a persistent search for novel redox species is necessary. Recently, the proton-coupled electron transfer (PCET) reaction of ruthenium complexes was reported to show a high Seebeck coefficient.[25] PCET reaction is an electron-exchange reaction associated with adding or eliminating protons. The large solvation entropy of the proton, which is strongly coordinated by water molecules, provides an arguably high Seebeck coefficient of 3.7 mV K^{-1}. However, these compounds are unsuitable for practical application due to the high cost of the ruthenium complexes. Moreover, the solubility of these complexes is extremely low (approx. 1 mM in the mixture of water and acetonitrile), which results in low carrier concentration, low carrier conductivity and low *ZT* value.

As an alternative redox pair that undergoes the PCET reaction, we focused on a vanadium aqua complex (Fig. 1). The vanadium aqua complex can be prepared by simple mixing of tetravalent (V^{4+}) and pentavalent vanadium (V^{5+}) salts. These vanadium complexes are widely used for redox-flow batteries[26,27] because of their high solubility and stability. Furthermore, the Pourbaix diagram of the vanadium complex (Fig. 2a) shows that the 1-electron-3-protons PCET reaction takes place in a pH range from 3 to 4 (Eq. 1).

$$[VO(H_2O)_3]^{2+} \rightleftarrows [VO(OH)_3]^0 + e^- + 3H^+ \qquad \text{(Eq. 1)}$$

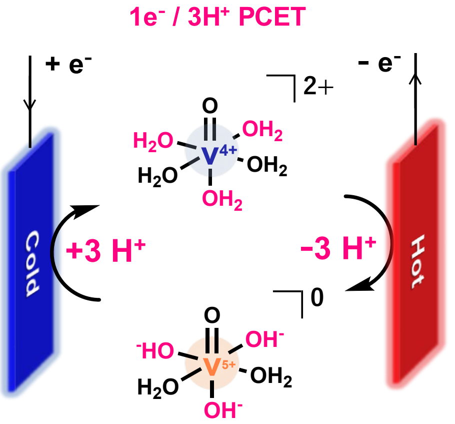

Figure 1. Schematic illustration of a TEC consisting of an aqueous electrolyte of $V^{4+/5+}$ that shows the 1e$^-$/3H$^+$ PCET reaction at pH 3–4. The temperature difference between the two electrodes of TEC promotes an entropy-increasing reaction on the hot side, and an entropy-decreasing reaction on the cold side, respectively. Reduction of the V^{5+} aqua complex causes protonation of the vanadium complex, which is promoted at the cold side electrode. The reverse reaction associated with the deprotonation of the complex occurs on the hot side.

---

[a] Department of Chemistry, Faculty of Science, The University of Tokyo, Hongo 7-3-1, Bunkyo-ku, Tokyo 113-0033, Japan.
[b] Department of Chemistry and Biochemistry, Graduate School of Engineering, Kyushu University, Motooka 744, Nishi-ku, Fukuoka 819-0035, Japan.
[c] Department of Chemistry, Graduate School of Science, Kyushu University.

Electronic Supplementary Information (ESI) available: [details of any supplementary information available should be included here]. See DOI: 10.1039/x0xx00000x

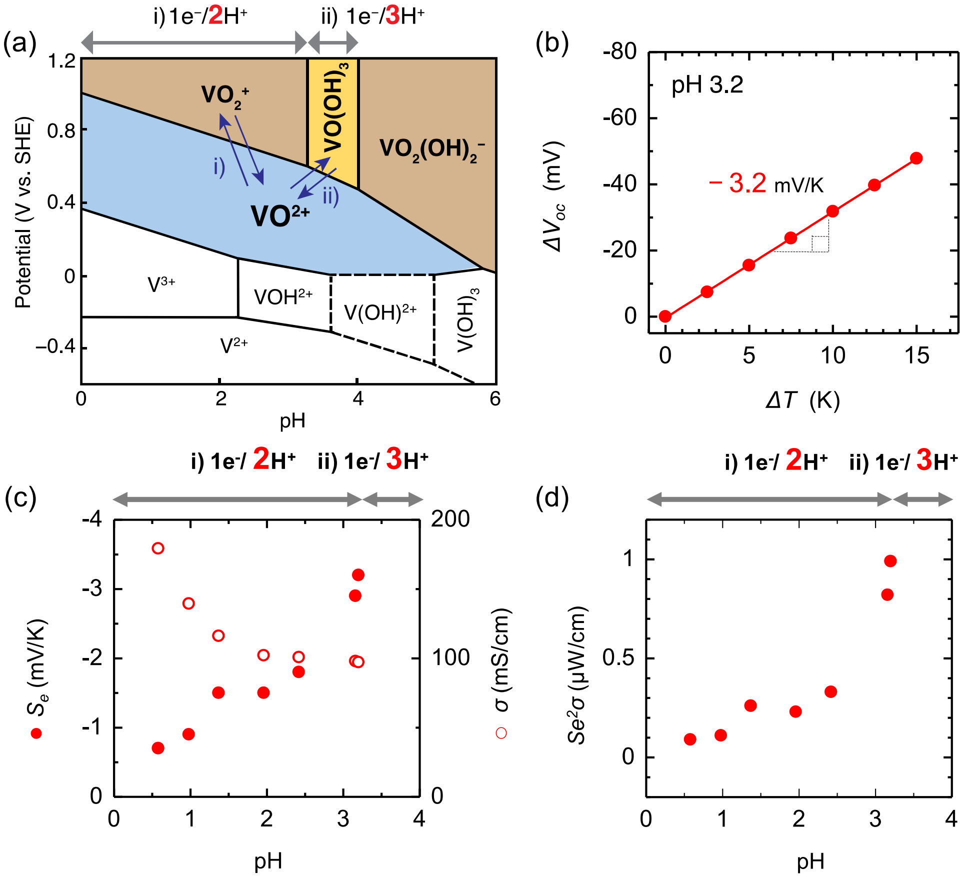

Figure 2. (a) Pourbaix diagram of vanadium aqua complex highlighting the two types of redox reactions of V^{4+} species (VO^{2+}) with V^{5+} species: i) with VO_2^+ at pH < 3; ii) with $VO(OH)_3$ at pH 3–4 (b) Plot of open-circuit voltage (ΔV_{oc}) and the temperature difference (ΔT) of a TEC containing 100 mM of $V^{4+/5+}$ ions in 3 M $NaHSO_4$ buffer at pH 3.2. The pH dependence of (c) Seebeck coefficient (S_e) and ionic conductivity (σ) and (d) σS_e^2 of the vanadium aqua TEC. The phase diagram is modified from the one reported in the literature[28].

According to the results and discussion of the previous report[25], the 1-electron-3-proton ($1e^-/3H^+$) provides tripled entropy change for the proton solvation per elemental charge, and thus high S_e is expected. Despite such a simple structure, there is no report on TECs using the vanadium aqua complex. In this manuscript, we report that the vanadium aqua TEC shows a high Seebeck coefficient due to the large change in entropy of the PCET reaction and high ionic conductivity (σ) because of the high carrier concentration. The estimated ZT value of the vanadium aqua TEC surpasses that of $[Fe(CN)_6]^{3-/4-}$, showing that the vanadium aqua complex is a promising material that could replace the benchmark redox pair used for TEC.

The redox equilibrium of the vanadium complexes was prepared by mixing vanadium oxide sulfate ($VOSO_4$) and vanadium oxide (V_2O_5) in an aqueous 3 M sodium hydrogen sulfate ($NaHSO_4$) buffer solution. The pH of the solution was adjusted by the addition of NaOH. The solution was filled in a custom-made H-shaped glass tube, and the two compartments were immersed in cold or hot water baths, respectively, and the temperature difference (ΔT) was recorded (Fig. S2). Two platinum wires were inserted into each cell compartment, and the potential difference between the wires was measured by a source meter. The cell's open-circuit voltage (ΔVoc) increased with the increasing temperature difference between the two electrodes (Fig. 2b). The S_e of the TEC was evaluated from the slope of the fitting line as −3.2 mV K^{-1}, comparable to the PCET redox pair of the ruthenium complex.[25]

The elimination of three protons from the vanadium complex is associated with one electron oxidation in the reaction (Eq. 1). In fact, the protons were captured by the base in the buffer solution, and sulfate is protonated and becomes hydrogen sulfate:

$$H^+ + SO_4^{2-} \rightleftharpoons HSO_4^- \qquad \text{(Eq. 2)}$$

The above equation can be rewritten as:

$$[\mathrm{VO(H_2O)_3}]^{2+} + 3\mathrm{SO_4^{2-}} \rightleftharpoons [\mathrm{VO(OH)_3}] + \mathrm{e}^- + 3\mathrm{HSO_4^-} \quad \text{(Eq. 3)}$$

The divalent SO_4^{2-} anion shows stronger solvation with water compared to the monovalent HSO_4^-. Thus, the oxidation reaction is more entropically-favorable and is promoted at a higher temperature. The oxidation reaction at the hot electrode should result in negative ΔV_{oc} values, which agrees with the experimental observation. The entropy change associated with Eq. 2 is 111.7 J mol^{-1} K^{-1},[29] corresponding to S_e of −1.2 mV K^{-1} per elimination of one proton. Because Eq. 3 is the $1e^-/3H^+$ PCET process, the tripled value (i.e., −3.6 mV K^{-1}) is expected and agrees with the experimental result (−3.2 mV K^{-1}).

The pH dependency of the S_e was investigated by varying the pH of the electrolyte. As shown in Fig. 2c, the S_e gradually increases with increasing pH from ca. −1 to ca. −2 mV K^{-1} up to approximately pH 3. According to the Pourbaix diagram of vanadium (Fig. 2a), $1e^-/2H^+$ type PCET reaction is dominant in the lower pH region, as shown in Eq 4.

$$[\mathrm{VO(H_2O)}]^{2+} \rightleftharpoons [\mathrm{VO_2}] + \mathrm{e}^- + 2\mathrm{H}^+ \quad \text{(Eq. 4)}$$

The smaller number of protons is associated with the reaction at that pH region, which results in a small S_e value. The S_e increased drastically to a maximum of −3.2 mV K^{-1} above pH 3, where the $1e^-/3H^+$ type PCET reaction takes place.

We previously reported that mixing of acetonitrile into the aqueous buffer solution increases S_e of the ruthenium PCET system.[25] A similar experiment was conducted using a mixture of water and acetonitrile solvents to compare the effect of the solvent on the S_e. The acetonitrile concentration varied from 0% (i.e. pure water) to 50% and 67%. The concentration of redox species was readjusted for each solution due to the change in solubility. For all the mixing ratios, a drastic increase of the S_e was observed from pH 2 to around pH 3 (Fig. S1, Supporting Information, SI). The increment of S_e became more pronounced with the higher concentration of acetonitrile. The maximum S_e of −3.8 mV K^{-1} was observed at acetonitrile concentration of 67%. This solvent dependence of S_e is comparable to that of the ruthenium TEC. These results indicate that the S_e of PCET reactions is strongly influenced by the solvent. Moreover, the solvation entropy is generally greater for smaller ionic radii of the redox ions, and structurally simple and small ligands such as water or ammonia can yield higher S_e than large organic ligands. However, our results show that the increment of S_e is comparable between the ruthenium complex with organic ligand and the vanadium aqua complexes. Therefore, the enhancement of S_e by PCET reaction is a versatile strategy regardless of the types of ligands.

The dimensionless figure of merit, *ZT* value, is regarded as the performance indicator and determined by the S_e, σ, and thermal conductivity (κ):

$$ZT = \frac{\sigma S_e^2 T}{\kappa} \quad \text{(Eq. 5)}$$

The σ of the TECs depends on the conductivity of both the oxidant and the reductant. The total conductivity was evaluated by the simple two-probe method as ca. 100 mS cm^{-1} at pH 3.2 (Fig. 2d). This high conductivity is nearly two orders of magnitude higher than that in the previous report with the ruthenium complex. This high conductivity reflects the increase in the concentration of redox species. The current–voltage (*I*–*V*) curve shows that the maximum power is ca. 180 nW (Fig. 3a), which is more than ten times higher than the previous result obtained with the ruthenium complex in the same setup, indicating that the improved ionic conductivity results in higher power output. The κ was evaluated as 0.62 W m^{-1} K^{-1}, agreeing with the value of common aqueous solutions. The *ZT* value is estimated as 4.7×10^{-1}, which is 25 times greater than the previously obtained result with the ruthenium complexes. Moreover, it is 2.5 times higher than the *ZT* of $[Fe(CN)_6]^{3-/4-}$ (Table S1, SI). When we compare the parameters, the concentration of redox species in the conventional $[Fe(CN)_6]^{3-/4-}$ TEC is higher than that in the vanadium aqua TEC, resulting in a conductivity twice that of the vanadium system. On the other hand, the S_e of the $[Fe(CN)_6]^{3-/4-}$ TEC is less than half of the value of vanadium aqua TEC. Therefore, the overall value of *ZT* and the power output of the vanadium system is more than twice that of $[Fe(CN)_6]^{3-/4-}$ because the *ZT* value is proportional to the square of S_e. This result suggests that the vanadium TEC could be considered as a novel benchmark of TECs. It is to note that the vanadium TEC has a limit in the applicable pH region. A mild acidic condition is necessary for a $1e^-/3H^+$ type PCET reaction. The applicable pH range of the vanadium TEC is different from the conventional $[Fe(CN)_6]^{3-/4-}$ TEC, which can decompose and release toxic hydrogen cyanide gas under acidic conditions. Therefore, these two TECs find application in different pH ranges where they can make use of their respective characteristics.

The electrochemical Peltier effect is the reverse process of the TEC, where electrode temperature changes by applying constant external current.[30,31] The aqueous $V^{4+/5+}$ electrolyte was adjusted to pH 2.8 because of the better stability of the solution, compared to the same electrolyte at pH 3.2, in which a small amount of precipitation was observed after a few hours. The temperature of the platinum electrode was reduced by −10 mK after 40 seconds of application of 1 mA cm^{-2} (Fig. 3b). This cooling effect was comparable to or even slightly greater than the benchmark $[Fe(CN)_6]^{3-/4-}$ redox pair, showing that the aqueous $V^{4+/5+}$ solution is a promising electrolyte for the electrochemical refrigeration.

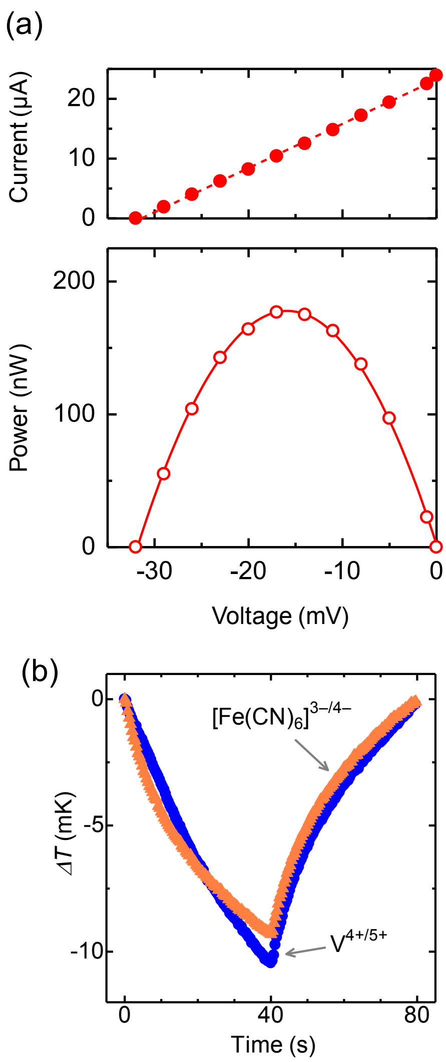

Figure 3. (a) Current–voltage (top) and power–voltage (bottom) plots of $1e^-/3H^+$ PCET reaction of vanadium aqua TEC. ΔT was maintained at c.a. 10 K. (b) Electrochemical Peltier cooling of aqueous $V^{4+/5+}$ redox pair (50 mM, pH 2.8). A constant current of ±1 mA cm^{-2} was applied with the current direction switched every 40 seconds, and the ΔT of the electrode after 500 cycles was averaged. The result of $[Fe(CN)_6]^{3-/4-}$ redox pair (400 mM) is supplied for comparison.

In summary, we investigated the thermoelectric conversion performance of TEC consisting of a vanadium aqua complex. The vanadium aqua TEC shows a high S_e of −3.2 mV K^{-1} in water and −3.8 mV K^{-1} in a mixture of acetonitrile and water. The S_e is dependent on pH, indicating that the $1e^-/3H^+$ type PCET reaction plays an important role. In contrast to the previous TEC system using the ruthenium complexes, the vanadium aqua complex exhibits higher solubility in water, resulting in arguably high ionic conductivity. As a result, the ZT value of this vanadium system exceeds that of the $[Fe(CN)_6]^{3-/4-}$ system in terms of the physical parameters of the electrolyte (i.e., the combination of S_e, σ, and κ). With regards to the recent drastic improvement in the output power of $[Fe(CN)_6]^{3-/4-}$ system achieved by using high-surface-area electrodes[5], such a significant improvement in power is also expected in the present system. The double ZT value compared to $[Fe(CN)_6]^{3-/4-}$ is expected to be a critical step toward the practical application of TECs.

Author Contributions

TY, NK and HZ supervised the data acquisition and processing. TK and TY wrote the original manuscript and NK and HZ edited the manuscript. TK, YW, FM and KY conducted the experiments and analyzed the data.

Conflicts of interest

There are no conflicts to declare.

Acknowledgements

This work was supported by JSPS KAKENHI Grant Numbers: 21H00017 (Hydrogenomics), 20H02714; 21K20527, 21K04949, 21H05870, 20K21176, JST CREST Grant Number: JPMJCR22O5, the Murata Science Foundation, The Asahi Glass Foundation, Tanikawa Fund Promotion of Thermal Technology, Yamada Science Foundation, The Iwatani Naoji Foundation, and the Canon Foundation.

Notes and references

1 M. F. Dupont, D. R. MacFarlane and J. M. Pringle, Thermo-electrochemical cells for waste heat harvesting – progress and perspectives, 2017, **53**, 6288–6302.

2 Y. Liu, M. Cui, W. Ling, L. Cheng, H. Lei, W. Li and Y. Huang, Thermo-electrochemical cells for heat to electricity conversion: from mechanisms, materials, strategies to applications, *Energy & Environmental Science*, 2022, **15**, 3670–3687.

3 H. Zhou, H. Inoue, M. Ujita and T. Yamada, Advancement of Electrochemical Thermoelectric Conversion with Molecular Technology, *Angewandte Chemie International Edition*, 2023, **62**, e202213449.

4 T. J. Abraham, D. R. MacFarlane and J. M. Pringle, Seebeck coefficients in ionic liquids -prospects for thermo-electrochemical cells, *Chemical Communications*, 2011, **47**, 6260–6262.

5 L. Zhang, T. Kim, N. Li, T. J. Kang, J. Chen, J. M. Pringle, M. Zhang, A. H. Kazim, S. Fang, C. Haines, D. Al-Masri, B. A. Cola, J. M. Razal, J. Di, S. Beirne, D. R. MacFarlane, A. Gonzalez-Martin, S. Mathew, Y. H. Kim, G. Wallace and R. H. Baughman, High Power Density Electrochemical Thermocells for Inexpensively Harvesting Low-Grade Thermal Energy, *Advanced Materials*, 2017, **29**, 1605652.

6 B. Yu, J. Duan, H. Cong, W. Xie, R. Liu, X. Zhuang, H. Wang, B. Qi, M. Xu, Z. L. Wang and J. Zhou, Thermosensitive crystallization–boosted liquid thermocells for low-grade heat harvesting, *Science*, 2020, **370**, 342–346.

7 J. Duan, G. Feng, B. Yu, J. Li, M. Chen, P. Yang, J. Feng, K. Liu and J. Zhou, Aqueous thermogalvanic cells with a high Seebeck coefficient for low-grade heat harvest, *Nature Communications*, 2018, **9**, 5146.

8 T. I. Quickenden and C. F. Vernon, Thermogalvanic conversion of heat to electricity, *Solar Energy*, 1986, **36**, 63–72.

9 IkeshojiTamio and T. Ikeshoji, Thermoelectric Conversion by Thin-Layer Thermogalvanic Cells with Soluble Redox Couples, **60**, 1505–1514.

10 T. Ikeshoji, F. N. B. de Nahui, S. Kimura and M. Yoneya, Computer analysis on natural convection in thin-layer thermocells with a soluble redox couple: Part 2. E-I relation,

electric power, heat flux and electrochemical heat pump, *Journal of Electroanalytical Chemistry and Interfacial Electrochemistry*, 1991, **312**, 43–56.

11 B. Burrows, Discharge Behavior of Redox Thermogalvanic Cells, 1976, **123**, 154–159.

12 Y. Mua, T. I. Quickenden and Y. Mua, A Review of Power Generation in Aqueous Thermogalvanic Cells, 1995, **142**, 3985.

13 Y. Mua and T. I. Quickenden, Power Conversion Efficiency, Electrode Separation, and Overpotential in the Ferricyanide/Ferrocyanide Thermogalvanic Cell, *Journal of The Electrochemical Society*.

14 R. Hu, B. A. Cola, N. Haram, J. N. Barisci, S. Lee, S. Stoughton, G. Wallace, C. Too, M. Thomas, A. Gestos, M. E. dela Cruz, J. P. Ferraris, A. A. Zakhidov and R. H. Baughman, Harvesting Waste Thermal Energy Using a Carbon-Nanotube-Based Thermo-Electrochemical Cell, *Nano Letters*, 2010, **10**, 838–846.

15 T. J. Kang, S. Fang, M. E. Kozlov, C. S. Haines, N. Li, Y. H. Kim, Y. Chen and R. H. Baughman, Electrical Power From Nanotube and Graphene Electrochemical Thermal Energy Harvesters, *Advanced Functional Materials*, 2012, **22**, 477–489.

16 T. J. Abraham, D. R. MacFarlane and J. M. Pringle, High Seebeck coefficient redox ionic liquid electrolytes for thermal energy harvesting.

17 A. J. DeBethune, T. S. Licht and N. Swendeman, The Temperature Coefficients of Electrode Potentials: The Isothermal and Thermal CoefficientsmThe Standard Ionic Entropy of Electrochemical Transport of the Hydrogen Ion, *Journal of the Electrochemical Society*, 1959, **106**, 626–627.

18 Y. Ikeda, K. Fukui and Y. Murakami, Integration of thermo-electrochemical conversion into forced convection cooling, *Physical Chemistry Chemical Physics*, 2019, **21**, 25838–25848.

19 Y. Ikeda, Y. Cho and Y. Murakami, Thermogalvanic energy harvesting from forced convection cooling of 100–200 °C surfaces generating high power density, *Sustainable Energy & Fuels*, 2021, **5**, 5967–5974.

20 Y. Liang, T. Yamada, H. Zhou and N. Kimizuka, Hexakis(2,3,6-tri-O-methyl)-α-cyclodextrin–I5− Complex in Aqueous I−/I3− Thermocells and Enhancement in the Seebeck Coefficient, *Chemical Science*, 2019, **10**, 773–780.

21 H. Zhou, T. Yamada and N. Kimizuka, Supramolecular Thermocells Based on Thermo-Responsiveness of Host–Guest Chemistry, *https://doi.org/10.1246/bcsj.20210061*, 2021, **94**, 1525–1546.

22 B. Guo, Y. Hoshino, F. Gao, K. Hayashi, Y. Miura, N. Kimizuka and T. Yamada, Thermocells Driven by Phase Transition of Hydrogel Nanoparticles, *Journal of the American Chemical Society*, 2020, **142**, 17318–17322.

23 Y. Liang, J. K. H. Hui, T. Yamada and N. Kimizuka, Electrochemical Thermoelectric Conversion with Polysulfide as Redox Species, *ChemSusChem*, 2019, **12**, 4014–4020.

24 Y. Liang, H. Zhou, T. Yamada and N. Kimizuka, No Title, *Bulletin of the Chemical Society of Japan*, 2019, **92**, bcsj.20190062.

25 T. Kobayashi, T. Yamada, M. Tadokoro and N. Kimizuka, A Novel Thermocell System Using Proton Solvation Entropy, *Chemistry – A European Journal*, , DOI:10.1002/chem.202004562.

26 M. Skyllas-Kazacos, M. Rychcik, R. G. Robins, A. G. Fane and M. A. Green, New All-Vanadium Redox Flow Cell, *Journal of The Electrochemical Society*, 1986, **133**, 1057–1058.

27 W. Wang, Q. Luo, B. Li, X. Wei, L. Li and Z. Yang, Recent Progress in Redox Flow Battery Research and Development, *Advanced Functional Materials*, 2013, **23**, 970–986.

28 E. Del Carpio, L. Hernández, C. Ciangherotti, V. Villalobos Coa, L. Jiménez, V. Lubes and G. Lubes, Vanadium: History, chemistry, interactions with α-amino acids and potential therapeutic applications, *Coordination Chemistry Reviews*, 2018, **372**, 117–140.

29 D. D. Wagman, H. E. William, V. B. Parker, R. H. Schumm, I. Halow, S. M. Bailey, K. L. Churney and R. L. Nuttall, The NBS tables of chemical thermodynamic prperties selected values for inorganic and C1 and C2 organic substances in SI units, *Journal of Physical and Chemical Reference Data*.

30 I. S. McKay, L. Y. Kunz and A. Majumdar, Electrochemical Redox Refrigeration, *Scientific Reports*, 2019, **9**, 1–8.

31 A. Rajan, I. S. McKay and S. K. Yee, Continuous electrochemical refrigeration based on the Brayton cycle, *Nature Energy 2022 7:4*, 2022, **7**, 320–328.